

Beyond Freeze-Out: A Novel Freeze-in Mechanism for Dark Matter via Supercooled Phase Transitions

Seyed Yaser Ayazi*^{id}^a and Mojtaba Hosseini†^{id}^a

^aDepartment of Physics, Semnan University, P.O. Box 35131-19111, Semnan, Iran

February 21, 2025

Abstract

We investigate a novel freeze-in mechanism for Weakly Interacting Massive Particles (WIMPs), facilitated by a supercooled first-order phase transition (FOPT) in the early universe. Unlike the conventional freeze-out and freeze-in scenarios, this mechanism allows WIMPs to acquire their relic abundance through a non-equilibrium production process following a rapid entropy injection. We explore multiple dark matter (DM) candidates, including vector, fermionic, and scalar-mediated models, and identify fermionic DM with a pseudoscalar mediator as the most viable candidate for this mechanism. The study demonstrates that FOPT dilutes preexisting DM density and simultaneously induces a rapid mass increase, preventing thermal re-equilibration and enabling DM production via freeze-in. Additionally, we analyze the gravitational wave (GW) signals associated with FOPT, identifying parameter regions detectable by future GW observatories such as LISA and UDECIGO. This framework offers a compelling alternative to traditional WIMP and Feebly Interacting Massive Particle (FIMP) scenarios, providing new avenues for DM model building and experimental verification.

1 Introduction

The nature of DM remains one of the most profound mysteries in modern physics [1,2]. Despite overwhelming astrophysical and cosmological evidence for its existence, the particle identity of DM continues to elude discovery. The Standard Model of elementary particles (SM), despite its enormous success in describing nature in its most fundamental form, does not contain any candidates for DM. Therefore, the presence of models beyond the SM is essential to describe DM [3–58]. Among the many theoretical paradigms proposed to explain DM, WIMPs have been extensively studied, primarily through the well-established freeze-out mechanism [59–61]. In this scenario, WIMPs achieve thermal equilibrium in the early universe and decouple as the universe expands and cools. However, traditional WIMP models face challenges from stringent experimental constraints, motivating the exploration of alternative production mechanisms.

The freeze-in mechanism offers a compelling alternative, wherein DM particles are never in thermal equilibrium but are produced gradually from the interactions of particles in the thermal bath [62]. Freeze-in has historically been associated with FIMPs, which interact so weakly that their production rate is suppressed, resulting in a relic density that matches observations.

*syaser.ayazi@semnan.ac.ir

†mojtaba_hosseini@semnan.ac.ir

The role of FOPT and its impact on DM phenomenology is very important [63–96]. Recently, however, a novel variation of the freeze-in mechanism has been proposed for WIMPs, where weak or moderate interaction strengths suffice due to the influence of a supercooled FOPT in the early universe [97](Freeze-in of WIMP). This scenario opens a new path for DM model building, enabling WIMPs to remain a viable candidate while resolving challenges associated with traditional freeze-out. It provides a robust framework for exploring physics beyond the SM, including connections to FOPT and GW signals. This new mechanism suggests WIMPs can also freeze-in under certain conditions:

- A *supercooled first-order phase transition* dilutes preexisting DM density to near zero.
- The phase transition increases the mass of DM significantly, leading to a large mass-to-temperature ratio. This prevents WIMPs from re-equilibrating with the thermal bath.

Therefore, in the study of DM production in the early universe, two main mechanisms are commonly considered: the traditional WIMP freeze-out and FIMP freeze-in. These mechanisms differ in their interaction strengths, thermal equilibrium conditions, and the role of phase transitions. Freeze-out describes the decoupling of once-equilibrated DM particles, leading to their relic abundance. Traditional freeze-in applies to feebly interacting particles that never reached equilibrium but were gradually produced over cosmic history. The WIMP freeze-in provides a new connection between FOPT and DM, opening up a third possibility for realizing DM besides WIMPs and FIMPs. It can be tested by combining the WIMP and GW experiments.

This work explores the WIMP freeze-in production of various DM candidates facilitated by an FOPT. The FOPT provides two essential effects: the injection of entropy that dilutes preexisting DM and a rapid mass increase for DM particles, preventing thermal equilibration. While the scalar WIMP candidate is a natural choice for demonstrating this mechanism [97], it can be extended to several other DM candidates.

The paper is organised as follows. In section. 2, we extend SM by several different models and DM candidates. In section. 3, we examine the conditions of the WIMP freeze-in scenario and present the numerical analyses of the models in light of supercooled FOPT scenario and study production of GWs in section 4, respectively. Finally, the conclusions present in section. 5.

2 The models

In this section, we present different models with different DM candidates, for which we will examine the conditions of the Freeze-in of WIMP in the next section. These models are presented in Table 2.

2.1 Vector DM with $U(1)$ symmetry

The Lagrangian of this model is as follows [54, 55]:

$$\mathcal{L} = \mathcal{L}_{SM} - \frac{1}{4}V_{\mu\nu}V^{\mu\nu} + (D'_\mu S)^*(D'^\mu S) - V(H, S), \quad (2.1)$$

where \mathcal{L}_{SM} is the SM Lagrangian without the Higgs potential term and the covariant derivative and field strength of V_μ are given as:

$$\begin{aligned} D'_\mu S &= (\partial_\mu + ig_v V_\mu)S, \\ V_{\mu\nu} &= \partial_\mu V_\nu - \partial_\nu V_\mu. \end{aligned}$$

The potential which is renormalizable and invariant under gauge and Z_2 symmetry is:

$$V(H, S) = -\mu_H^2 H^\dagger H - \mu_S^2 S^* S + \lambda_H (H^\dagger H)^2 + \lambda_S (S^* S)^2 + \lambda_{SH} (S^* S)(H^\dagger H). \quad (2.2)$$

Due to the imposed Z_2 symmetry under which only the dark gauge boson V_μ is odd, the vector field V_μ can be considered as a DM candidate. The S field is the intermediate between the dark sector and the SM sector. After the electroweak symmetry breaking, the parameters of the model are given by:

$$\begin{aligned} \nu_2 &= \frac{M_V}{g_v}, & \sin \alpha &= \frac{\nu_1}{\sqrt{\nu_1^2 + \nu_2^2}} \\ \lambda_H &= \frac{\cos^2 \alpha M_{H_1}^2 + \sin^2 \alpha M_{H_2}^2}{2\nu_1^2} \\ \lambda_S &= \frac{\sin^2 \alpha M_{H_1}^2 + \cos^2 \alpha M_{H_2}^2}{2\nu_2^2} \\ \lambda_{SH} &= \frac{(M_{H_2}^2 - M_{H_1}^2) \sin \alpha \cos \alpha}{\nu_1 \nu_2} \end{aligned} \quad (2.3)$$

Where the model includes three independent parameters M_V , M_{H_2} and g_v .

2.2 Scale Invariant Vector DM with $U(1)$ symmetry

In this model, there is no mass term at the tree level, and electroweak symmetry breaking occurs at the one-loop level via the Gildener- Weinberg mechanism [98]. The Lagrangian of this model is as follows [56, 99]:

$$\mathcal{L} = \mathcal{L}_{SM} + (D'_\mu S)^*(D'^\mu S) - V(H, S) - \frac{1}{4} V_{\mu\nu} V^{\mu\nu}, \quad (2.4)$$

where \mathcal{L}_{SM} is the SM Lagrangian without the Higgs potential term and

$$\begin{aligned} D'_\mu S &= (\partial_\mu + ig_v V_\mu)S, \\ V_{\mu\nu} &= \partial_\mu V_\nu - \partial_\nu V_\mu. \end{aligned}$$

The most general scale-invariant potential which is renormalizable and invariant under gauge and Z_2 symmetry is:

$$V(H, S) = \frac{\lambda_H}{6} (H^\dagger H)^2 + \frac{\lambda_S}{6} (S^* S)^2 + 2\lambda_{SH} (S^* S)(H^\dagger H). \quad (2.5)$$

Similar to the previous model, the vector field V_μ is a candidate for DM and S is the intermediate between the dark sector and the SM. After the symmetry breaking, we have the following

constraints:

$$\begin{aligned}
\nu_2 &= \frac{M_V}{g_v}, & \sin\alpha &= \frac{\nu_1}{\sqrt{\nu_1^2 + \nu_2^2}} \\
\lambda_H &= \frac{3M_{H_1}^2}{\nu_1^2} \cos^2\alpha, & \lambda_S &= \frac{3M_{H_1}^2}{\nu_2^2} \sin^2\alpha \\
\lambda_{SH} &= -\frac{M_{H_1}^2}{2\nu_1\nu_2} \sin\alpha \cos\alpha, & &
\end{aligned} \tag{2.6}$$

where M_V is the mass of vector DM after symmetry breaking. Regarding one-loop effect, the dark Higgs mass is given by [56, 98]

$$M_{H_2}^2 = \frac{1}{8\pi^2\nu^2} (M_{H_1}^4 + 6M_W^4 + 3M_Z^4 + 3M_V^4 - 12M_t^4), \tag{2.7}$$

where $M_{W,Z,t}$ are the masses of W, Z gauge bosons, and top quark, respectively. Constraints (2.6) severely restrict free parameters of the model up to two independent parameters of M_V and g_v .

2.3 Fermionic DM with $U(1)$ symmetry

This model is also scale invariant and symmetry breaking occurs at the one-loop level. The model contains three new fields: a vector field V_μ , a Dirac fermion field ψ that can play the role of DM and a complex scalar S , mediates between SM and the dark sector. In the model V_μ , ψ and S are charged under a new dark $U(1)_D$ gauge group and all of these fields are singlet under SM gauge groups. The $U(1)_D$ charge of the new particles are given in Table 1. The Lagrangian of this model is as follows [53]:

$$\mathcal{L} = \mathcal{L}_{SM} + i\bar{\psi}_L\gamma^\mu D_\mu\psi_L + i\bar{\psi}_R\gamma^\mu D_\mu\psi_R - g_s\bar{\psi}_L\psi_R S + h.c. - \frac{1}{4}V_{\mu\nu}V^{\mu\nu} + (D_\mu S)^*(D^\mu S) - V(H, S). \tag{2.8}$$

where \mathcal{L}_{SM} is the SM Lagrangian without the Higgs potential term, The covariant derivative is

$$\begin{aligned}
D_\mu &= (\partial_\mu + iQg_v V_\mu), \quad \text{and} \\
V_{\mu\nu} &= \partial_\mu V_\nu - \partial_\nu V_\mu,
\end{aligned} \tag{2.9}$$

where Q is the charge of the new particles under $U(1)$ symmetry. The most general scale-invariant potential $V(H, S)$ that is renormalizable and invariant under gauge symmetry is

$$V(H, S) = \frac{1}{6}\lambda_H(H^\dagger H)^2 + \frac{1}{6}\lambda_S(S^* S)^2 + 2\lambda_{SH}(S^* S)(H^\dagger H). \tag{2.10}$$

After the symmetry breaking, we have the following constraints:

$$\begin{aligned}
\nu_2 &= \frac{M_V}{g_v}, & \sin\alpha &= \frac{\nu_1}{\sqrt{\nu_1^2 + \nu_2^2}} \\
M_\psi &= \frac{g_s M_V}{\sqrt{2}g_v}, & \lambda_H &= \frac{3M_{H_1}^2}{\nu_1^2} \cos^2\alpha \\
\lambda_S &= \frac{3M_{H_1}^2}{\nu_2^2} \sin^2\alpha, & \lambda_{SH} &= -\frac{M_{H_1}^2}{2\nu_1\nu_2} \sin\alpha \cos\alpha,
\end{aligned} \tag{2.11}$$

Field	S	ψ_L	ψ_R
$U(1)_D$ charge	1	$\frac{1}{2}$	$-\frac{1}{2}$

Table 1: The charges of the dark sector particles under the new $U(1)_D$ symmetry.

where M_ψ and M_V are the masses of vector and fermion fields after symmetry breaking. Meanwhile, since we do not assume $M_V < 2M_\psi$, the only candidate for DM is ψ . Regarding one-loop effect, the dark Higgs mass is given by [98]:

$$M_{H_2}^2 = \frac{1}{8\pi^2\nu^2} (M_{H_1}^4 + 6M_W^4 + 3M_Z^4 + 3M_V^4 - 12M_t^4 - 4M_\psi^4). \quad (2.12)$$

where $M_{W,Z,t}$ are the masses of W, Z gauge bosons, and top quark, respectively. In the equations above, H_1 is the Higgs boson and $M_{H_1} = 125$ GeV. According to (2.11), the independent parameters of the model are M_V , M_ψ and the coupling g_v .

2.4 Fermionic DM with scalar mediator vs. pseudoscalar mediator

In this model, the SM is extended with two new fields: a Dirac fermion ψ which plays the role of the DM candidate and a (pseudo)scalar field S that interacts with the DM through a Yukawa term. The Lagrangian of the model is as follows [100]:

$$\mathcal{L} = \mathcal{L}_{SM} + \mathcal{L}_{dark}(\psi, S) + \mathcal{L}_S(S) + \mathcal{L}_{int}(H, S, \psi), \quad (2.13)$$

where \mathcal{L}_{SM} stands for the SM Lagrangian. The Lagrangian of fermionic DM, $\mathcal{L}_{dark}(\psi, S)$, is :

$$\mathcal{L}_{dark}(\psi, S) = \bar{\psi}(i\gamma_\mu\partial^\mu - M_\psi)\psi. \quad (2.14)$$

\mathcal{L}_S is as follows:

$$\mathcal{L}_S = \frac{1}{2}(\partial^\mu S)^2 - \frac{1}{2}\mu_S^2 S^2 - \frac{1}{4}\lambda_S S^4, \quad (2.15)$$

and \mathcal{L}_{int} is the (pseudo)scalar interaction with the dark and the SM sectors. When S is a pseudoscalar then,

$$\mathcal{L}_{int}(H, S, \psi) = g_d S \bar{\psi} \gamma^5 \psi + \frac{1}{2} \lambda_{SH} S^2 H^\dagger H, \quad (2.16)$$

and when S represents the scalar,

$$\mathcal{L}_{int}(H, S, \psi) = g_d S \bar{\psi} \psi + \frac{1}{2} \lambda_{SH} S^2 H^\dagger H. \quad (2.17)$$

The Higgs potential in the SM sector reads:

$$V_H = -\mu_H^2 H^\dagger H - \lambda_H (H^\dagger H)^2. \quad (2.18)$$

The tree-level potential which is given by the substitution $H = (0 \ h \equiv \langle h_1 \rangle)^\dagger$ and $S \equiv \langle h_2 \rangle$ reads,

$$V_0(h_1, h_2) = -\frac{1}{2}\mu_H^2 h_1^2 - \frac{1}{2}\mu_S^2 h_2^2 + \frac{1}{4}\lambda_H h_1^4 + \frac{1}{4}\lambda_S h_2^4 + \frac{1}{2}\lambda_{SH} h_1^2 h_2^2. \quad (2.19)$$

After the symmetry breaking both Higgs particle and the scalar field undergo non-zero vev . In fact, by substituting $h_1 \rightarrow \nu_1 + h_1$ and $h_2 \rightarrow \nu_2 + h_2$, the fields h_1 and h_2 mix with each other and they can be rewritten by the mass eigenstates H_1 and H_2 as

$$\begin{aligned} H_1 &= h_1 \cos \theta + h_2 \sin \theta, \\ H_2 &= -h_1 \sin \theta + h_2 \cos \theta. \end{aligned} \quad (2.20)$$

In the above equations, θ is the mixing angle. In the following we assume that H_1 is the eigenstate of the SM Higgs with $M_{H_1} = 125$ GeV ($\nu_1 = 246$ GeV) and H_2 corresponds to the eigenstate of the singlet scalar. After symmetry breaking, we have

$$\begin{aligned} \lambda_H &= \frac{M_{H_2}^2 \sin^2 \theta + M_{H_1}^2 \cos^2 \theta}{2\nu_1^2} \\ \lambda_S &= \frac{M_{H_2}^2 \cos^2 \theta + M_{H_1}^2 \sin^2 \theta}{2\nu_2^2} \\ \lambda_{SH} &= \frac{(M_{H_2}^2 - M_{H_1}^2) \sin 2\theta}{2\nu_1 \nu_2} \end{aligned} \quad (2.21)$$

According to the above equations, the independent parameters of the model can be chosen as $M_{H_2}, M_\psi, \theta, g_d$ and ν_2 . Note that all we have said in this section is true for both scalar and pseudoscalar mediators.

Models	Symmetry	Key Parameters
Vector DM with $U(1)$ symmetry	$U(1)$	M_V, M_{H_2}, g_v
Scale Invariant Vector DM with $U(1)$ symmetry	$U(1)$	M_V, g_v
Fermionic DM with $U(1)$ symmetry	$U(1)$	M_V, M_ψ, g_v
Fermionic DM with Scalar Mediator	Z_2	$M_{H_2}, M_\psi, \theta, g_d, \nu_2$
Fermionic DM with Pseudoscalar Mediator	Z_2	$M_{H_2}, M_\psi, \theta, g_d, \nu_2$

Table 2: Summary of DM models, their symmetries, and key parameters.

3 Freeze-in of WIMP

Freeze-in of WIMP is a novel scenario for producing DM that is the boundary between freeze-out and freeze-in mechanisms [97]. In this mechanism, in the conventional thermal history of the Universe, DM particles inevitably thermalize and freeze-out. Freeze-in of WIMPs can happen if the Universe experiences a supercooled FOPT. A supercooled FOPT releases a huge amount of entropy, which dilutes the preexisting DM density to a negligible level. The WIMPs gain mass from the FOPT and never return to equilibrium due to their large mass-to-temperature ratio. After the FOPT, DM will be accumulatively produced via the process of $SM SM \rightarrow DM DM$, which is a typical freeze-in scenario, but it applies to weak or moderate couplings. The main point of this introduced mechanism is that the coupling between the dark side and the SM is larger than the conventional freeze-in case.

In the early universe, $DM(X)$ was massless and $z \equiv (M_X/T) = 0$. With the start of supercooling at temperature T_2 , the DM mass undergoes a sudden change to $M_X \gg T_2$, where

T_2 denotes the temperature after the FOPT. We assume a supercooled FOPT such that $T_2 \gg T_1$. T_1 is the temperature at which the FOPT begins. This leads to an enormous increase in entropy density by a factor of $(T_2/T_1)^3$ and dilutes the preexisting DM density to a negligible level. Consequently, the evolution of the density of DM begins at $z_2 = M_X/T_2 \gg 1$, with an initial condition $Y_X(z_2) \approx (T_1/T_2)^3 Y_1 \sim 0$. From here on, the production of DM particles begins with the freeze-in mechanism and with a negligible initial amount.

With the above interpretations, the two basic conditions for establishing the presented scenario are as follows:

- **Reheating temperature T_2 must be greater than the critical temperature T_1 ($T_2 \gg T_1$):**

In this scenario, T_2 (reheating temperature) must always be greater than T_1 . T_Λ is the temperature at which supercooling(starting a phase of thermal inflation) begins and when reheating is prompt ($\Gamma \gg H$), we have [63,101]:

$$T_2 = T_\Lambda = \left(\frac{30V_\Lambda}{\pi^2 g_*}\right)^{\frac{1}{4}}. \quad (3.1)$$

In the above equation, $g_* \approx 106.75$ and for all models presented in the paper, $\Gamma \gg H$, where Γ is the decay width of scalars and H is the Hubble constant during the FOPT. The V_Λ quantity is also defined as follows [63]:

$$V_\Lambda = \frac{\beta_{\lambda_S} v_2^4}{16}, \quad (3.2)$$

where v_2 is the vacuum expectation value of the scalar mediator S and β_{λ_S} is the one-loop beta function for coupling of scalar mediator λ_S . In the following, we examine this condition for all the presented models.

1. The Model 2.1 :

This model includes three independent parameters M_V , M_{H_2} and g_v . For this model, all possible phase transition states have been investigated in reference [102]. In this case, there is no phase transition, either one-step or two-step, that can be observed in consistent with the DM constraints, including the correct relic density of DM [103]. Therefore, this model cannot be included in the mechanism proposed for the production of DM in this paper.

2. The Model 2.2 :

This model includes two independent parameters M_V and g_v . According to equation 2.7, M_V must always be greater than 240 GeV. Figure 1 shows the behavior of critical temperature(T_1) and reheating temperature(T_2) for different couplings and masses. As can be seen, only for a very small portion of the parameter space($240 \text{ GeV} < M_V < 500 \text{ GeV}$), T_2 is larger than T_1 . But to establish the mechanism of Freeze-in of WIMP, we must assume that $T_2 \gg T_1$, which is not the case here, and both temperatures are very close and $T_2/T_1 \sim 1$. Therefore, this model cannot be included in the framework of the presented mechanism.

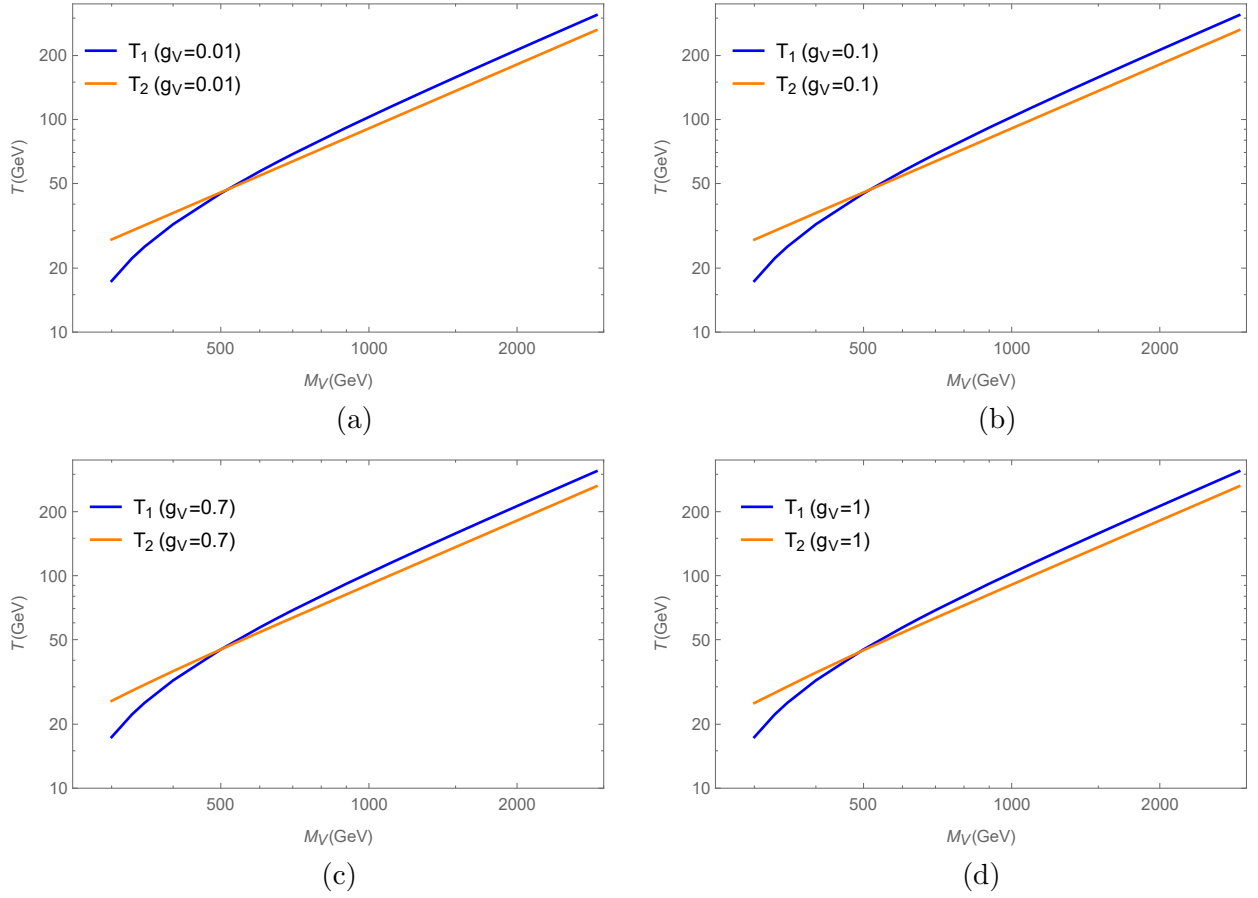


Figure 1: Temperature variations for the model 2.2 with respect to DM mass for different couplings.

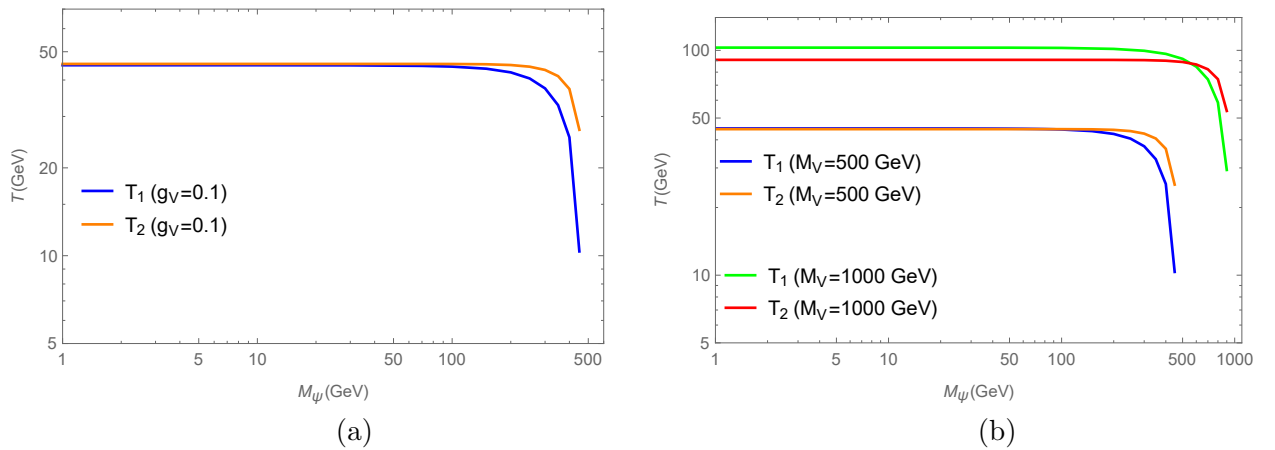


Figure 2: Temperature variations for the model 2.3 with respect to DM mass. In (a) $M_V = 500$ GeV and in (b) $g_V = 1$ is considered. We know that in the model must always $M_\psi < M_V/2$ so that the only DM particle in the model is the fermion ψ .

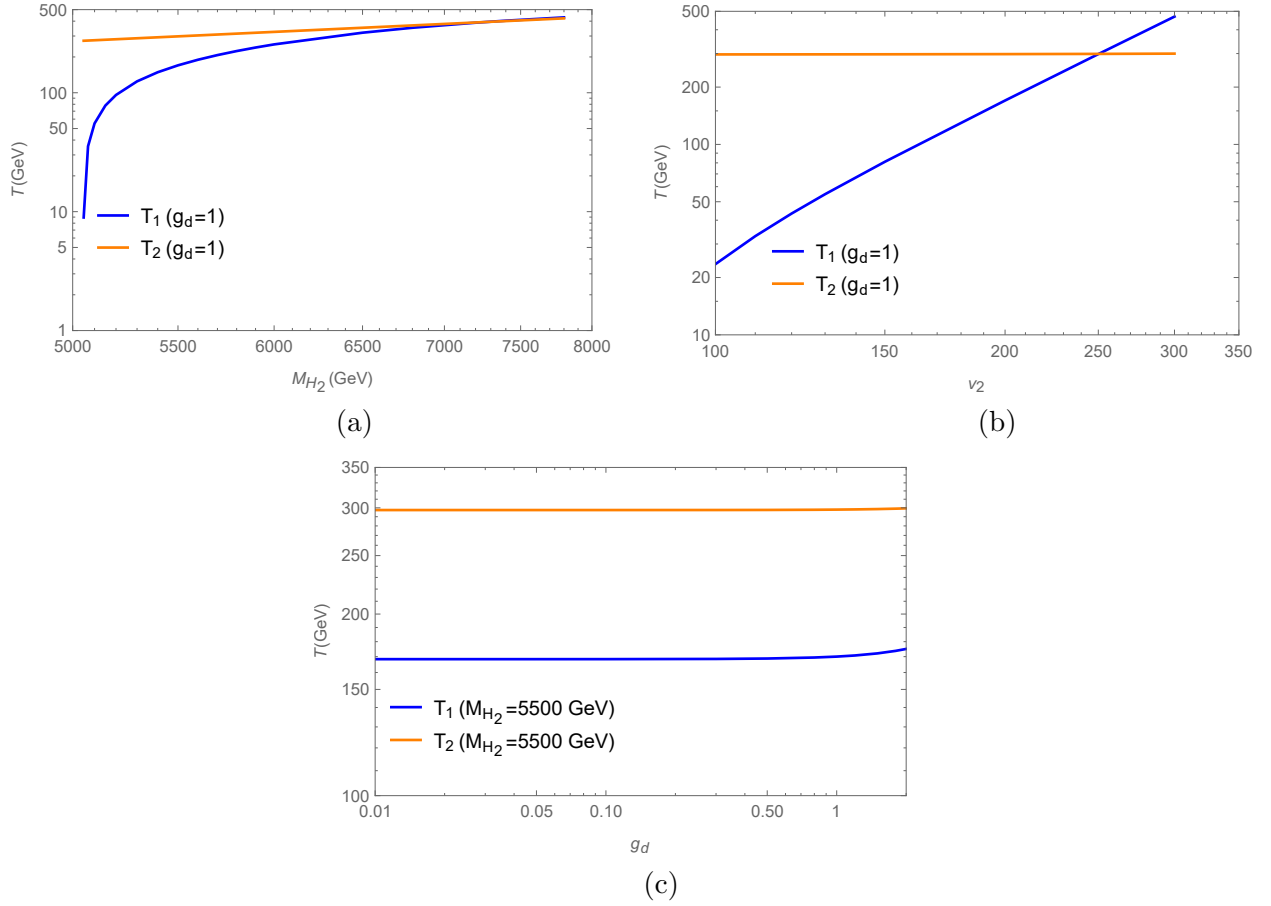


Figure 3: Temperature variations with respect to the independent parameters of the model 2.4. The mixing angle is assumed $\theta = 1^\circ$. In (a) $v_2 = 200$ GeV, in (b) $M_{H_2} = 5500$ GeV and in (c) $M_{H_2} = 5500$ GeV and $v_2 = 200$ GeV is considered.

3. The Model 2.3 :

This model includes three independent parameters M_V , M_ψ and g_v . First, it is important to note that in the model, for our only candidate for DM to be a fermionic particle(ψ), we must have $M_\psi < M_V/2$. In Figure 2(a), temperature changes are plotted against the mass of DM for constant g_v and M_V . As can be seen, $T_2 \sim T_1$ and $T_2/T_1 \sim 1$. But from $M_\psi > 250$ GeV, T_2 will be a relatively large distance from T_1 , which is not the case in the model scenario where only the fermionic particle is a candidate for DM($M_\psi < M_V/2 = 250$ GeV). In Figure 2(b), temperature changes are plotted for different M_V . As can be seen, as M_V increases, T_2 becomes smaller than T_1 . But for smaller M_V , T_2 becomes a relatively significant distance from T_1 at a point where the single-component DM condition(only ψ as a DM candidate) in the model is violated(because of $M_\psi > M_V/2$). Therefore, this model like the previous two models cannot be included in the framework of the presented mechanism.

4. The Model 2.4 :

Since the model 2.4 with scalar mediator is very limited and it has been publicly ruled out by direct discovery experiments [100], we examine Model 2.4 with pseudoscalar mediator. By choosing the mediator in the model 2.4 to be a pseudoscalar [100], the elastic scattering cross section for DM-nucleon is velocity suppressed and so the theory easily evades the direct detection bounds from XENONnT and LZ [104, 105]. There are five independent parameters $M_{H_2}, M_\psi, \theta, g_d$ and ν_2 in this model. An overall result of the Higgs signal strength measured by ATLAS and CMS will restrict the Higgs mixing angle to values smaller than $\sin \theta \leq 0.12$ ($\theta \leq 6.9^\circ$) [106]. Therefore, in the rest of the paper we consider the mixing angle($\theta = 1^\circ$). Also, the mass of DM(M_ψ) will not have any effect on determining the temperatures T_1 and T_2 . In Figure 3(a), temperature changes are plotted against the mass of H_2 for constant g_d and ν_2 . As can be seen, as the M_{H_2} decreases, T_2 will become much larger than T_1 , and $\frac{T_2}{T_1} \gg 1$. In Figure 3(b), temperature changes are plotted against the ν_2 for constant g_d and M_{H_2} . As can be seen, as the ν_2 decreases, T_2 will become much larger than T_1 . In Figure 3(c), temperature changes are plotted against the g_d for constant ν_2 and M_{H_2} . As can be seen, T_2 is always greater than T_1 , but their changes are constant with g_d . As a result, the two determining parameters for examining temperatures are M_{H_2} and ν_2 . Therefore, this model has the initial condition $T_2 \gg T_1$ for the mechanism of freeze-in of WIMP and allows for the examination of this mechanism. It can also be protected from strong constraints of direct detection.

In Figure 4, the allowed parameter space is also plotted in consistent with the constraint of $T_2 > T_1$ for independent parameters of model. A summary of the analysis performed in this section is provided in Table 3.

So according the above points, we conclude that only fermionic dark matter with a pseudo scalar mediator satisfies the condition of $T_2 \gg T_1$. The supercooled FOPT enables freeze-in WIMP production specifically for it due to a combination of unique conditions and constraints

that are satisfied only in this scenario. Here's a detailed explanation:

1. **Entropy Injection and Dilution of Preexisting DM:** A supercooled FOPT releases a significant amount of entropy into the universe. This entropy injection dilutes any preexisting DM density to nearly zero. This is a crucial condition for the freeze-in mechanism, as it ensures that the DM production starts from a negligible initial abundance. For fermionic DM with a pseudoscalar mediator, this dilution is particularly effective because the pseudoscalar mediator allows for a specific type of interaction that can maintain the DM out of thermal equilibrium after the phase transition.
2. **Mass Increase and Suppression of Thermal Equilibration:** During the FOPT, the mass of the DM particles increases significantly. This large mass-to-temperature ratio prevents the DM particles from re-equilibrating with the thermal bath after the phase transition. In the case of fermionic DM with a pseudoscalar mediator, the mass increase is such that the DM particles remain out of equilibrium, which is essential for the freeze-in mechanism to operate. The pseudoscalar mediator facilitates this by providing a coupling that is weak enough to prevent re-equilibration but strong enough to allow for gradual DM production.

Models	Condition of $T_2 \gg T_1$
Vector DM with $U(1)$ symmetry	Impossible
Scale Invariant Vector DM with $U(1)$ symmetry	Impossible
Fermionic DM with $U(1)$ symmetry	Impossible
Fermionic DM with Scalar Mediator	Impossible
Fermionic DM with Pseudoscalar Mediator	Possible

Table 3: Condition of $T_2 \gg T_1$ for different models

- **Failure to return to equilibrium conditions after FOPT ($T_2 < T_{dec}$):**

In this scenario, for $T_2 > T_{dec}$, the plasma thermalizes again, and the usual freeze-out mechanism yields the relic abundance [63, 101]. $T_{dec} \sim M_{DM}/25$ is temperature of freeze-out. So we are looking for points in the parameter space where $T_2 < T_{dec}$. Consequently, the evolution of Boltzmann equation begins at $z_2 = M_{DM}/T_2 \gg 1$ where the equation is as follows:

$$\frac{dY_X}{dz} = -\sqrt{\frac{\pi g_{*,s}^2}{45 g_*}} \frac{M_{Pl} M_X}{z^2} \langle \sigma \nu_{rel} \rangle (Y_X^2 - Y_{eq}^2), \quad (3.3)$$

where $Y_X = n_X/s$ is the yield of X with s being the entropy density, $z = M_X/T$, $M_{Pl} = 1.22 \times 10^{19}$ GeV is the Planck scale, $g_{*,s}$ and g_* are the numbers the relativistic degrees of freedom for entropy and energy, respectively. $\sigma \nu_{rel}$ is the thermal average of the annihilation cross section multiplying the relative velocity ν_{rel} under the Maxwell-Boltzmann distribution, and $K_i(z)$ is the i -th modified Bessel function. Finally, the allowable parameter space according to the Freeze-in WIMP mechanism is plotted in Figure 5.

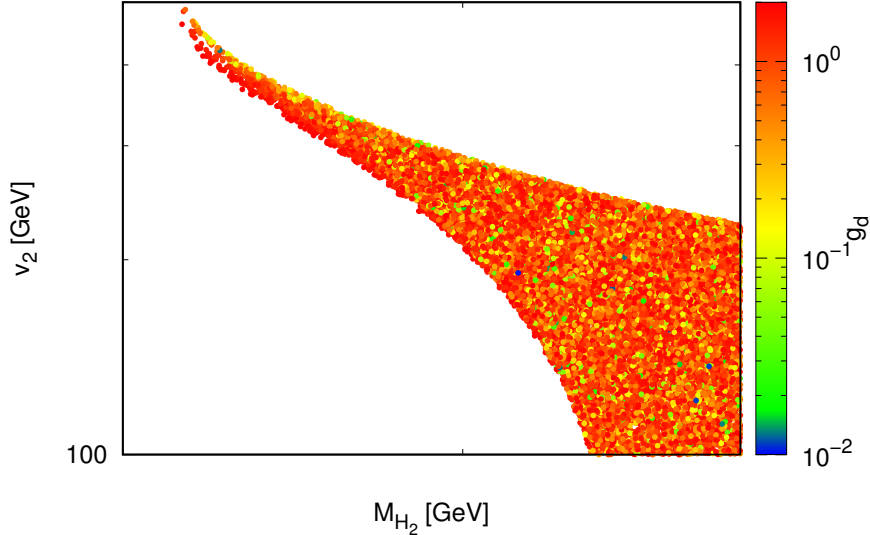


Figure 4: Allowed parameter space in agreement with the condition of $T_2 > T_1$ for the model 2.4 with pseudoscalar mediator. The mixing angle is assumed $\theta = 1^\circ$. Our scan is done with $4000 \text{ GeV} < M_{H_2} < 6000 \text{ GeV}$, $100 \text{ GeV} < \nu_2 < 500 \text{ GeV}$, and the dark coupling in the range $0.01 < g_d < 2$.

These points are in consistent with the observed relic density of DM [103]. The conditions of $T_2 \gg T_1$ and $T_2 < T_{dec}$ hold for all points. For these points, z_2 is between 26 and 32. Of course, we know that M_ψ is the mass of DM.

4 Gravitational wave signals

The total thermal effective potential is as follows [53]:

$$V_{eff} = V_0(h_1, h_2) + V_{1-loop}(h_1, h_2; 0) + V_{1-loop}(h_1, h_2; T), \quad (4.1)$$

where V_0 is the tree-level potential in eq.2.19, $V_{1-loop}(h_1, h_2; 0)$ is the Coleman-Weinberg one-loop correction at zero temperature [107] and $V_{1-loop}(h_1, h_2; T)$ is the one-loop thermal correction [108]. In the high-temperature approximation, the one-loop effective potential takes the following form:

$$V_{1-loop}^{high-T}(h_1, h_2; T) = \left(\frac{1}{2} \kappa_{h_1} h_1^2 + \frac{1}{2} \kappa_{h_2} h_2^2 \right) T^2, \quad (4.2)$$

in which we have

$$\kappa_{h_1} = \frac{1}{48} (9g_1^2 + 3g_2^2 + 12g_t^2 + 24\lambda_H + 4\lambda_{SH}), \quad (4.3)$$

$$\kappa_{h_2} = \frac{1}{12} (4\lambda_{SH} + 3\lambda_S - g_d^2). \quad (4.4)$$

We have dropped the Colman-Wienberg zero-temperature correction since at high temperature approximation only the thermal corrections are dominant. In eq.4.3 the parameters g_1 and g_2 are respectively the $SU(2)_L$ and $U(1)_Y$ SM couplings and g_t is the top quark coupling.

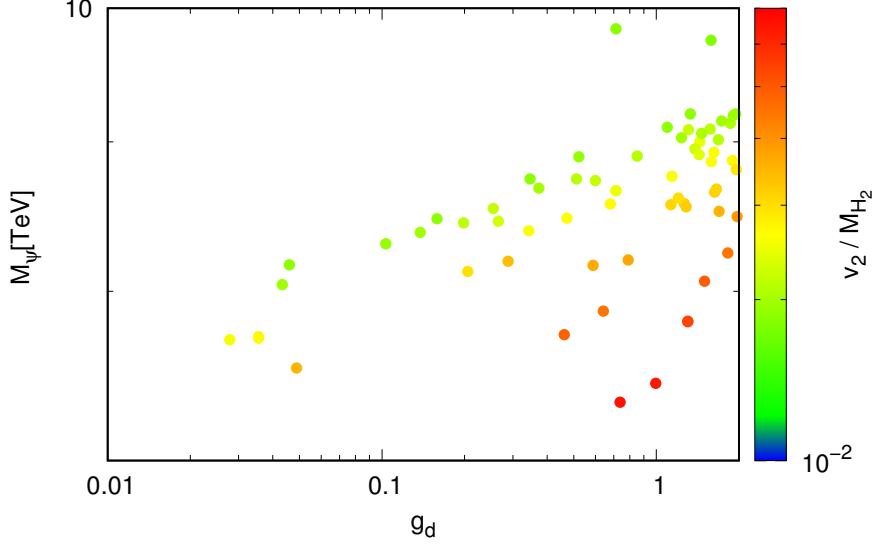


Figure 5: The parameter space that realizes the WIMP freeze-in scenario for model with pseudoscalar mediator. These points are in consistent with the observed relic density of DM, $T_2 \gg T_1$ and $T_2 < T_{dec}$. The mixing angle is assumed $\theta = 1^\circ$. Our scan is done with $7 \text{ TeV} < M_\psi < 10 \text{ TeV}$, $100 \text{ GeV} < \nu_2 < 200 \text{ GeV}$, $4500 \text{ GeV} < M_{H_2} < 6000 \text{ GeV}$ and the dark coupling in the range $0.01 < g_d < 2$.

We use the potential 4.1 to calculate GWs from the model. In the case of significant supercooling, the GW signal arises from bubble collisions [101]. To calculate the GW spectra, we need the phase transition strength α , inverse phase transition duration β/H_* , v_ω and $T_*(T_2)$. The bubble collision contribution to the spectrum of GW in the our scenario is given by [109, 110]:

$$\Omega_{coll}(f)h^2 = 1.67 \times 10^{-5} \left(\frac{T_2}{T_\Lambda}\right)^{4/3} \left(\frac{\beta}{H_*}\right)^{-2} \left(\frac{\kappa\alpha}{1+\alpha}\right)^2 \left(\frac{g_*}{100}\right)^{-\frac{1}{3}} \left(\frac{0.11v_\omega^3}{0.42+v_\omega^2}\right) S_{coll}, \quad (4.5)$$

where S_{coll} parametrises the spectral shape and is given by

$$S_{coll} = \frac{3.8(f/f_{coll})^{2.8}}{2.8(f/f_{coll})^{3.8} + 1}, \quad (4.6)$$

where

$$f_{coll} = 1.65 \times 10^{-5} \left(\frac{T_2}{T_\Lambda}\right)^{1/3} \left(\frac{0.62}{v_\omega^2 - 0.1v_\omega + 1.8}\right) \left(\frac{\beta}{H_*}\right) \left(\frac{T_\Lambda}{100}\right) \left(\frac{g_*}{100}\right)^{1/6} Hz. \quad (4.7)$$

The α and β/H_* parameters are as follows [111]:

$$\alpha = \frac{\Delta\left(V_{eff} - T\frac{\partial V_{eff}}{\partial T}\right)\Big|_{T_*}}{\rho_*}, \quad (4.8)$$

$$\frac{\beta}{H_*} = T_* \frac{d}{dT} \left(\frac{S_3(T)}{T}\right)\Big|_{T_*}, \quad (4.9)$$

where ρ_* is

$$\rho_* = \frac{\pi^2 g_*}{30} T_N^4. \quad (4.10)$$

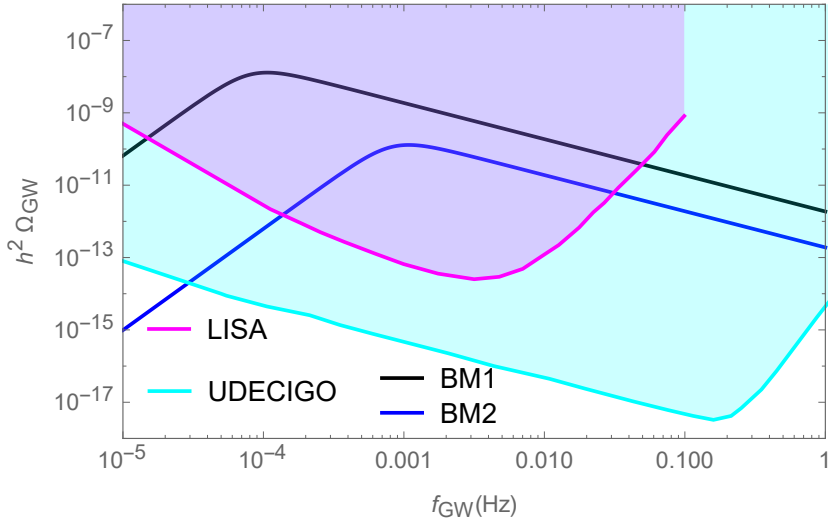


Figure 6: GW spectrum for benchmark points of the Table 4.

The velocity of the bubble wall (v_w) which is anticipated to be close to 1 for the strong transitions [112] and $g_* \sim 100$ is the effective number of relativistic degrees of freedom in the thermal plasma. Figure 6 shows the gravitational wave spectrum for the parameters given in table 4. As can be seen, the peak of this spectrum will fall within the range of the LISA and UDECIGO experiments [111, 113].

	M_ψ (GeV)	g_d	ν_2 (GeV)	M_{H_2} (GeV)	T_2 (GeV)	T_1 (GeV)	α	β/H_*
1	8573	1.26	164.57	5198.14	281.42	1.49	4.05×10^8	10
2	8390	0.34	140.96	5297.67	286.09	1.5	2.27×10^9	100

Table 4: Input and output parameters for two benchmark points.

5 Conclusion

In the paper, we explored a generalized freeze-in mechanism for DM production, leveraging the effects of a supercooled FOPT. We demonstrated that the entropy injection and mass increase associated with FOPT create conditions that allow WIMPs to undergo freeze-in rather than the conventional freeze-out mechanism. Our study considered multiple DM candidates, including vector, fermionic, and scalar-mediated DM models, identifying scenarios where freeze-in is a viable production mechanism.

Among the models examined, we found that a fermionic DM scenario with a pseudoscalar mediator best satisfies the required conditions for WIMP freeze-in, particularly in maintaining out-of-equilibrium dynamics post-FOPT. This model provides a unique framework where DM relic abundance can be generated with moderate couplings, making it distinct from traditional freeze-in models that typically involve extremely feeble interactions.

Additionally, we analyzed the GW signals associated with the supercooled FOPT, identifying parameter regions where the predicted GW spectra fall within the sensitivity ranges of future experiments such as LISA and UDECIGO. These findings highlight the potential for upcoming GW observations to probe new physics related to DM production.

Overall, this study establishes WIMP freeze-in as a robust and unifying framework for DM model building, offering new perspectives on DM candidates beyond conventional thermal histories. Future research may focus on refining parameter constraints through collider and GW observations, further solidifying the role of FOPT in shaping the early universe's DM dynamics.

References

- [1] G. Bertone and D. Hooper, *History of dark matter*, *Rev. Mod. Phys.* **90** (2018) 045002 [[1605.04909](#)].
- [2] M. Cirelli, A. Strumia and J. Zupan, *Dark Matter*, [2406.01705](#).
- [3] K. M. Zurek, *Multi-Component Dark Matter*, *Phys. Rev. D* **79** (2009) 115002 [[0811.4429](#)].
- [4] S. Profumo, K. Sigurdson and L. Ubaldi, *Can we discover multi-component WIMP dark matter?*, *JCAP* **12** (2009) 016 [[0907.4374](#)].
- [5] M. Aoki, M. Duerr, J. Kubo and H. Takano, *Multi-Component Dark Matter Systems and Their Observation Prospects*, *Phys. Rev. D* **86** (2012) 076015 [[1207.3318](#)].
- [6] A. Biswas, D. Majumdar, A. Sil and P. Bhattacharjee, *Two Component Dark Matter : A Possible Explanation of 130 GeV γ - Ray Line from the Galactic Centre*, *JCAP* **12** (2013) 049 [[1301.3668](#)].
- [7] P.-H. Gu, *Multi-component dark matter with magnetic moments for Fermi-LAT gamma-ray line*, *Phys. Dark Univ.* **2** (2013) 35 [[1301.4368](#)].
- [8] M. Aoki, J. Kubo and H. Takano, *Two-loop radiative seesaw mechanism with multicomponent dark matter explaining the possible γ excess in the Higgs boson decay and at the Fermi LAT*, *Phys. Rev. D* **87** (2013) 116001 [[1302.3936](#)].
- [9] Y. Kajiyama, H. Okada and T. Toma, *Multicomponent dark matter particles in a two-loop neutrino model*, *Phys. Rev. D* **88** (2013) 015029 [[1303.7356](#)].
- [10] L. Bian, R. Ding and B. Zhu, *Two Component Higgs-Portal Dark Matter*, *Phys. Lett. B* **728** (2014) 105 [[1308.3851](#)].
- [11] S. Bhattacharya, A. Drozd, B. Grzadkowski and J. Wudka, *Two-Component Dark Matter*, *JHEP* **10** (2013) 158 [[1309.2986](#)].
- [12] C.-Q. Geng, D. Huang and L.-H. Tsai, *Imprint of multicomponent dark matter on AMS-02*, *Phys. Rev. D* **89** (2014) 055021 [[1312.0366](#)].

- [13] S. Esch, M. Klasen and C. E. Yaguna, *A minimal model for two-component dark matter*, *JHEP* **09** (2014) 108 [[1406.0617](#)].
- [14] K. R. Dienes, J. Kumar, B. Thomas and D. Yaylali, *Dark-Matter Decay as a Complementary Probe of Multicomponent Dark Sectors*, *Phys. Rev. Lett.* **114** (2015) 051301 [[1406.4868](#)].
- [15] L. Bian, T. Li, J. Shu and X.-C. Wang, *Two component dark matter with multi-Higgs portals*, *JHEP* **03** (2015) 126 [[1412.5443](#)].
- [16] C.-Q. Geng, D. Huang and C. Lai, *Revisiting multicomponent dark matter with new AMS-02 data*, *Phys. Rev. D* **91** (2015) 095006 [[1411.4450](#)].
- [17] A. DiFranzo and G. Mohlabeng, *Multi-component Dark Matter through a Radiative Higgs Portal*, *JHEP* **01** (2017) 080 [[1610.07606](#)].
- [18] M. Aoki and T. Toma, *Implications of Two-component Dark Matter Induced by Forbidden Channels and Thermal Freeze-out*, *JCAP* **01** (2017) 042 [[1611.06746](#)].
- [19] A. Dutta Banik, M. Pandey, D. Majumdar and A. Biswas, *Two component WIMP–FIMP dark matter model with singlet fermion, scalar and pseudo scalar*, *Eur. Phys. J. C* **77** (2017) 657 [[1612.08621](#)].
- [20] M. Pandey, D. Majumdar and K. P. Modak, *Two Component Feebly Interacting Massive Particle (FIMP) Dark Matter*, *JCAP* **06** (2018) 023 [[1709.05955](#)].
- [21] D. Borah, A. Dasgupta, U. K. Dey, S. Patra and G. Tomar, *Multi-component Fermionic Dark Matter and IceCube PeV scale Neutrinos in Left-Right Model with Gauge Unification*, *JHEP* **09** (2017) 005 [[1704.04138](#)].
- [22] J. Herrero-Garcia, A. Scaffidi, M. White and A. G. Williams, *On the direct detection of multi-component dark matter: sensitivity studies and parameter estimation*, *JCAP* **11** (2017) 021 [[1709.01945](#)].
- [23] A. Ahmed, M. Duch, B. Grzadkowski and M. Igllicki, *Multi-Component Dark Matter: the vector and fermion case*, *Eur. Phys. J. C* **78** (2018) 905 [[1710.01853](#)].
- [24] S. Peyman Zakeri, S. Mohammad Moosavi Nejad, M. Zakeri and S. Yaser Ayazi, *A Minimal Model For Two-Component FIMP Dark Matter: A Basic Search*, *Chin. Phys. C* **42** (2018) 073101 [[1801.09115](#)].
- [25] M. Aoki and T. Toma, *Boosted Self-interacting Dark Matter in a Multi-component Dark Matter Model*, *JCAP* **10** (2018) 020 [[1806.09154](#)].
- [26] S. Chakraborti and P. Poulose, *Interplay of Scalar and Fermionic Components in a Multi-component Dark Matter Scenario*, *Eur. Phys. J. C* **79** (2019) 420 [[1808.01979](#)].
- [27] N. Bernal, D. Restrepo, C. Yaguna and O. Zapata, *Two-component dark matter and a massless neutrino in a new $B - L$ model*, *Phys. Rev. D* **99** (2019) 015038 [[1808.03352](#)].

- [28] A. Poulin and S. Godfrey, *Multicomponent dark matter from a hidden gauged $SU(3)$* , *Phys. Rev. D* **99** (2019) 076008 [[1808.04901](#)].
- [29] J. Herrero-Garcia, A. Scaffidi, M. White and A. G. Williams, *On the direct detection of multi-component dark matter: implications of the relic abundance*, *JCAP* **01** (2019) 008 [[1809.06881](#)].
- [30] S. Yaser Ayazi and A. Mohamadnejad, *Scale-Invariant Two Component Dark Matter*, *Eur. Phys. J. C* **79** (2019) 140 [[1808.08706](#)].
- [31] F. Elahi and S. Khatibi, *Multi-Component Dark Matter in a Non-Abelian Dark Sector*, *Phys. Rev. D* **100** (2019) 015019 [[1902.04384](#)].
- [32] D. Borah, A. Dasgupta and S. K. Kang, *Two-component dark matter withogenesis of the baryon asymmetry of the Universe*, *Phys. Rev. D* **100** (2019) 103502 [[1903.10516](#)].
- [33] D. Borah, R. Roshan and A. Sil, *Minimal two-component scalar doublet dark matter with radiative neutrino mass*, *Phys. Rev. D* **100** (2019) 055027 [[1904.04837](#)].
- [34] S. Bhattacharya, P. Ghosh, A. K. Saha and A. Sil, *Two component dark matter with inert Higgs doublet: neutrino mass, high scale validity and collider searches*, *JHEP* **03** (2020) 090 [[1905.12583](#)].
- [35] A. Biswas, D. Borah and D. Nanda, *Type III seesaw for neutrino masses in $U(1)_{B-L}$ model with multi-component dark matter*, *JHEP* **12** (2019) 109 [[1908.04308](#)].
- [36] D. Nanda and D. Borah, *Connecting Light Dirac Neutrinos to a Multi-component Dark Matter Scenario in Gauged $B - L$ Model*, *Eur. Phys. J. C* **80** (2020) 557 [[1911.04703](#)].
- [37] C. E. Yaguna and O. Zapata, *Multi-component scalar dark matter from a Z_N symmetry: a systematic analysis*, *JHEP* **03** (2020) 109 [[1911.05515](#)].
- [38] G. Bélanger, A. Pukhov, C. E. Yaguna and O. Zapata, *The Z_5 model of two-component dark matter*, *JHEP* **09** (2020) 030 [[2006.14922](#)].
- [39] P. Van Dong, C. H. Nam and D. Van Loi, *Canonical seesaw implication for two-component dark matter*, *Phys. Rev. D* **103** (2021) 095016 [[2007.08957](#)].
- [40] S. Khalil, S. Moretti, D. Rojas-Ciofalo and H. Waltari, *Multicomponent dark matter in a simplified E_6 SSM*, *Phys. Rev. D* **102** (2020) 075039 [[2007.10966](#)].
- [41] A. Dutta Banik, R. Roshan and A. Sil, *Two component singlet-triplet scalar dark matter and electroweak vacuum stability*, *Phys. Rev. D* **103** (2021) 075001 [[2009.01262](#)].
- [42] J. Hernandez-Sanchez, V. Keus, S. Moretti, D. Rojas-Ciofalo and D. Sokolowska, *Complementary Probes of Two-component Dark Matter*, [2012.11621](#).
- [43] N. Chakrabarty, R. Roshan and A. Sil, *Two-component doublet-triplet scalar dark matter stabilizing the electroweak vacuum*, *Phys. Rev. D* **105** (2022) 115010 [[2102.06032](#)].

- [44] C. E. Yaguna and O. Zapata, *Two-component scalar dark matter in Z_{2n} scenarios*, *JHEP* **10** (2021) 185 [2106.11889].
- [45] B. Díaz Sáez, P. Escalona, S. Norero and A. R. Zerwekh, *Fermion singlet dark matter in a pseudoscalar dark matter portal*, *JHEP* **10** (2021) 233 [2105.04255].
- [46] B. Díaz Sáez, K. Möhling and D. Stöckinger, *Two real scalar WIMP model in the assisted freeze-out scenario*, *JCAP* **10** (2021) 027 [2103.17064].
- [47] A. Mohamadnejad, *Electroweak phase transition and gravitational waves in a two-component dark matter model*, *JHEP* **03** (2022) 188 [2111.04342].
- [48] C. E. Yaguna and O. Zapata, *Fermion and scalar two-component dark matter from a Z_4 symmetry*, *Phys. Rev. D* **105** (2022) 095026 [2112.07020].
- [49] S.-Y. Ho, P. Ko and C.-T. Lu, *Scalar and fermion two-component SIMP dark matter with an accidental Z_4 symmetry*, *JHEP* **03** (2022) 005 [2201.06856].
- [50] Y. G. Kim, K. Y. Lee and S.-h. Nam, *Phenomenology of a two-component dark matter model*, *Phys. Lett. B* **834** (2022) 137412 [2201.11485].
- [51] A. Das, S. Gola, S. Mandal and N. Sinha, *Two-component scalar and fermionic dark matter candidates in a generic $U(1)X$ model*, *Phys. Lett. B* **829** (2022) 137117 [2202.01443].
- [52] G. Bélanger, A. Pukhov, C. E. Yaguna and O. Zapata, *The Z_7 model of three-component scalar dark matter*, *JHEP* **03** (2023) 100 [2212.07488].
- [53] M. Hosseini, S. Yaser Ayazi and A. Mohamadnejad, *Gravitational wave effects and phenomenology of a two-component dark matter model*, *Eur. Phys. J. C* **84** (2024) 485 [2308.00395].
- [54] S. Yaser Ayazi, M. Hosseini, S. Paktinat Mehdiabadi and R. Rouzbehi, *Vector dark matter and LHC constraints, including a 95 GeV light Higgs boson*, *Phys. Rev. D* **110** (2024) 055004 [2405.01132].
- [55] S. Yaser Ayazi and M. Hosseini, *W-boson mass anomaly and vacuum structure in vector dark matter model with a singlet scalar mediator*, *Int. J. Mod. Phys. A* **38** (2023) 2340002 [2206.11041].
- [56] S. Yaser Ayazi and A. Mohamadnejad, *Conformal vector dark matter and strongly first-order electroweak phase transition*, *JHEP* **03** (2019) 181 [1901.04168].
- [57] S. Yaser Ayazi, M. Hosseini and R. Rouzbehi, *Gravitational wave signatures of first-order phase transition in two-component dark matter model*, *Phys. Rev. D* **110** (2024) 115027 [2407.10123].
- [58] M. H. R. Abkenar, A. Mohamadnejad and R. Sepahvand, *Spin Trio: a dark matter scenario*, 2410.22252.

- [59] J. L. Feng, *The WIMP paradigm: Theme and variations*, *SciPost Phys. Lect. Notes* **71** (2023) 1 [2212.02479].
- [60] L. Roszkowski, E. M. Sessolo and S. Trojanowski, *WIMP dark matter candidates and searches—current status and future prospects*, *Rept. Prog. Phys.* **81** (2018) 066201 [1707.06277].
- [61] G. Arcadi, M. Dutra, P. Ghosh, M. Lindner, Y. Mambrini, M. Pierre et al., *The waning of the WIMP? A review of models, searches, and constraints*, *Eur. Phys. J. C* **78** (2018) 203 [1703.07364].
- [62] L. J. Hall, K. Jedamzik, J. March-Russell and S. M. West, *Freeze-In Production of FIMP Dark Matter*, *JHEP* **03** (2010) 080 [0911.1120].
- [63] T. Hambye, A. Strumia and D. Teresi, *Super-cool Dark Matter*, *JHEP* **08** (2018) 188 [1805.01473].
- [64] M. J. Baker, J. Kopp and A. J. Long, *Filtered Dark Matter at a First Order Phase Transition*, *Phys. Rev. Lett.* **125** (2020) 151102 [1912.02830].
- [65] D. Chway, T. H. Jung and C. S. Shin, *Dark matter filtering-out effect during a first-order phase transition*, *Phys. Rev. D* **101** (2020) 095019 [1912.04238].
- [66] T. Cohen, D. E. Morrissey and A. Pierce, *Changes in Dark Matter Properties After Freeze-Out*, *Phys. Rev. D* **78** (2008) 111701 [0808.3994].
- [67] M. J. Baker, M. Breitbach, J. Kopp and L. Mitnacht, *Dynamic Freeze-In: Impact of Thermal Masses and Cosmological Phase Transitions on Dark Matter Production*, *JHEP* **03** (2018) 114 [1712.03962].
- [68] L. Bian and Y.-L. Tang, *Thermally modified sterile neutrino portal dark matter and gravitational waves from phase transition: The Freeze-in case*, *JHEP* **12** (2018) 006 [1810.03172].
- [69] L. Bian and X. Liu, *Two-step strongly first-order electroweak phase transition modified FIMP dark matter, gravitational wave signals, and the neutrino mass*, *Phys. Rev. D* **99** (2019) 055003 [1811.03279].
- [70] M. J. Baker and J. Kopp, *Dark Matter Decay between Phase Transitions at the Weak Scale*, *Phys. Rev. Lett.* **119** (2017) 061801 [1608.07578].
- [71] A. Kobakhidze, M. A. Schmidt and M. Talia, *Mechanism for dark matter depopulation*, *Phys. Rev. D* **98** (2018) 095026 [1712.05170].
- [72] M. J. Baker and L. Mitnacht, *Variations on the Vev Flip-Flop: Instantaneous Freeze-out and Decaying Dark Matter*, *JHEP* **05** (2019) 070 [1811.03101].
- [73] P. Di Bari, D. Marfatia and Y.-L. Zhou, *Gravitational waves from neutrino mass and dark matter genesis*, *Phys. Rev. D* **102** (2020) 095017 [2001.07637].

- [74] A. Kobakhidze, M. A. Schmidt and M. Talia, *Thermal dark matter abundance under non-standard macroscopic conditions in the early universe*, *JCAP* **03** (2020) 059 [[1910.01433](#)].
- [75] A. Falkowski and J. M. No, *Non-thermal Dark Matter Production from the Electroweak Phase Transition: Multi-TeV WIMPs and 'Baby-Zillas'*, *JHEP* **02** (2013) 034 [[1211.5615](#)].
- [76] I. Baldes, Y. Gouttenoire and F. Sala, *String Fragmentation in Supercooled Confinement and Implications for Dark Matter*, *JHEP* **04** (2021) 278 [[2007.08440](#)].
- [77] A. Azatov, M. Vanvlasselaer and W. Yin, *Dark Matter production from relativistic bubble walls*, *JHEP* **03** (2021) 288 [[2101.05721](#)].
- [78] I. Baldes, Y. Gouttenoire and F. Sala, *Hot and heavy dark matter from a weak scale phase transition*, *SciPost Phys.* **14** (2023) 033 [[2207.05096](#)].
- [79] I. Baldes, Y. Gouttenoire, F. Sala and G. Servant, *Supercool composite Dark Matter beyond 100 TeV*, *JHEP* **07** (2022) 084 [[2110.13926](#)].
- [80] S. Roy, *Dilution of dark matter relic abundance due to first order electroweak phase transition in the singlet scalar extended type-II seesaw model*, *Phys. Rev. D* **111** (2025) 015037 [[2212.11230](#)].
- [81] E. Krylov, A. Levin and V. Rubakov, *Cosmological phase transition, baryon asymmetry and dark matter Q-balls*, *Phys. Rev. D* **87** (2013) 083528 [[1301.0354](#)].
- [82] F. P. Huang and C. S. Li, *Probing the baryogenesis and dark matter relaxed in phase transition by gravitational waves and colliders*, *Phys. Rev. D* **96** (2017) 095028 [[1709.09691](#)].
- [83] Y. Bai and A. J. Long, *Six Flavor Quark Matter*, *JHEP* **06** (2018) 072 [[1804.10249](#)].
- [84] Y. Bai, A. J. Long and S. Lu, *Dark Quark Nuggets*, *Phys. Rev. D* **99** (2019) 055047 [[1810.04360](#)].
- [85] A. Atreya, A. Sarkar and A. M. Srivastava, *Reviving quark nuggets as a candidate for dark matter*, *Phys. Rev. D* **90** (2014) 045010 [[1405.6492](#)].
- [86] J.-P. Hong, S. Jung and K.-P. Xie, *Fermi-ball dark matter from a first-order phase transition*, *Phys. Rev. D* **102** (2020) 075028 [[2008.04430](#)].
- [87] M. J. Baker, M. Breitbach, J. Kopp and L. Mittnacht, *Primordial Black Holes from First-Order Cosmological Phase Transitions*, [2105.07481](#).
- [88] K. Kawana and K.-P. Xie, *Primordial black holes from a cosmic phase transition: The collapse of Fermi-balls*, *Phys. Lett. B* **824** (2022) 136791 [[2106.00111](#)].

- [89] J. Liu, L. Bian, R.-G. Cai, Z.-K. Guo and S.-J. Wang, *Primordial black hole production during first-order phase transitions*, *Phys. Rev. D* **105** (2022) L021303 [[2106.05637](#)].
- [90] M. J. Baker, M. Breitbach, J. Kopp and L. Mittnacht, *Detailed Calculation of Primordial Black Hole Formation During First-Order Cosmological Phase Transitions*, [2110.00005](#).
- [91] K. Hashino, S. Kanemura and T. Takahashi, *Primordial black holes as a probe of strongly first-order electroweak phase transition*, *Phys. Lett. B* **833** (2022) 137261 [[2111.13099](#)].
- [92] P. Huang and K.-P. Xie, *Primordial black holes from an electroweak phase transition*, *Phys. Rev. D* **105** (2022) 115033 [[2201.07243](#)].
- [93] Y. Bai, S. Lu and N. Orlofsky, *Origin of nontopological soliton dark matter: solitosynthesis or phase transition*, *JHEP* **10** (2022) 181 [[2208.12290](#)].
- [94] K. Kawana, P. Lu and K.-P. Xie, *First-order phase transition and fate of false vacuum remnants*, *JCAP* **10** (2022) 030 [[2206.09923](#)].
- [95] S. He, L. Li, Z. Li and S.-J. Wang, *Gravitational waves and primordial black hole productions from gluodynamics by holography*, *Sci. China Phys. Mech. Astron.* **67** (2024) 240411 [[2210.14094](#)].
- [96] I. Baldes, M. Dichtl, Y. Gouttenoire and F. Sala, *Ultra-high-Energy Particle Collisions and Heavy Dark Matter at Phase Transitions*, *Phys. Rev. Lett.* **134** (2025) 061001 [[2306.15555](#)].
- [97] X.-R. Wong and K.-P. Xie, *Freeze-in of WIMP dark matter*, *Phys. Rev. D* **108** (2023) 055035 [[2304.00908](#)].
- [98] E. Gildener and S. Weinberg, *Symmetry Breaking and Scalar Bosons*, *Phys. Rev. D* **13** (1976) 3333.
- [99] M. Hosseini, S. Y. Ayazi and A. Mohamadnejad, *Gravitational wave in a filtered vector dark matter model*, [2405.10662](#).
- [100] P. H. Ghorbani, *Electroweak Baryogenesis and Dark Matter via a Pseudoscalar vs. Scalar*, *JHEP* **08** (2017) 058 [[1703.06506](#)].
- [101] D. Marfatia and P.-Y. Tseng, *Gravitational wave signals of dark matter freeze-out*, *JHEP* **02** (2021) 022 [[2006.07313](#)].
- [102] K. Hashino, M. Kakizaki, S. Kanemura, P. Ko and T. Matsui, *Gravitational waves from first order electroweak phase transition in models with the $U(1)_X$ gauge symmetry*, *JHEP* **06** (2018) 088 [[1802.02947](#)].
- [103] PLANCK collaboration, *Planck 2018 results. VI. Cosmological parameters*, *Astron. Astrophys.* **641** (2020) A6 [[1807.06209](#)].

- [104] XENON collaboration, *First Dark Matter Search with Nuclear Recoils from the XENONnT Experiment*, *Phys. Rev. Lett.* **131** (2023) 041003 [[2303.14729](#)].
- [105] LZ collaboration, *First Dark Matter Search Results from the LUX-ZEPLIN (LZ) Experiment*, *Phys. Rev. Lett.* **131** (2023) 041002 [[2207.03764](#)].
- [106] ATLAS, CMS collaboration, *Measurements of the Higgs boson production and decay rates and constraints on its couplings from a combined ATLAS and CMS analysis of the LHC pp collision data at $\sqrt{s} = 7$ and 8 TeV*, *JHEP* **08** (2016) 045 [[1606.02266](#)].
- [107] S. R. Coleman and E. J. Weinberg, *Radiative Corrections as the Origin of Spontaneous Symmetry Breaking*, *Phys. Rev. D* **7** (1973) 1888.
- [108] L. Dolan and R. Jackiw, *Symmetry Behavior at Finite Temperature*, *Phys. Rev. D* **9** (1974) 3320.
- [109] I. Baldes and C. Garcia-Cely, *Strong gravitational radiation from a simple dark matter model*, *JHEP* **05** (2019) 190 [[1809.01198](#)].
- [110] J. Ellis, M. Lewicki, J. M. No and V. Vaskonen, *Gravitational wave energy budget in strongly supercooled phase transitions*, *JCAP* **06** (2019) 024 [[1903.09642](#)].
- [111] C. Caprini et al., *Science with the space-based interferometer eLISA. II: Gravitational waves from cosmological phase transitions*, *JCAP* **04** (2016) 001 [[1512.06239](#)].
- [112] D. Bodeker and G. D. Moore, *Can electroweak bubble walls run away?*, *JCAP* **05** (2009) 009 [[0903.4099](#)].
- [113] K. Yagi and N. Seto, *Detector configuration of DECIGO/BBO and identification of cosmological neutron-star binaries*, *Phys. Rev. D* **83** (2011) 044011 [[1101.3940](#)].